De Novo Variants in *TAOK1* Cause Neurodevelopmental Disorders

Marija Dulovic-Mahlow,[1,13] Joanne Trinh,[1,13] Krishna Kumar Kandaswamy,[2] Geir Julius Braathen,[3] Nataliya Di Donato,[4] Elisa Rahikkala,[5,6] Skadi Beblo,[7,8] Martin Werber,[2] Victor Krajka,[1] Øyvind L. Busk,[3] Hauke Baumann,[1] Nouriya Abbas Al-Sannaa,[9] Frauke Hinrichs,[1] Rabea Affan,[10] Nir Navot,[10] Mohammed A. Al Balwi,[11] Gabriela Oprea,[2] Øystein L. Holla,[3] Maximilian E.R. Weiss,[2] Rami A. Jamra,[7] Anne-Karin Kahlert,[4] Shivendra Kishore,[2] Kristian Tveten,[3] Melissa Vos,[1,13] Arndt Rolfs,[2,12,13] and Katja Lohmann[1,13,*]

De novo variants represent a significant cause of neurodevelopmental delay and intellectual disability. A genetic basis can be identified in only half of individuals who have neurodevelopmental disorders (NDDs); this indicates that additional causes need to be elucidated. We compared the frequency of *de novo* variants in patient-parent trios with (n = 2,030) versus without (n = 2,755) NDDs. We identified *de novo* variants in *TAOK1* (thousand and one [TAO] amino acid kinase 1), which encodes the serine/threonine-protein kinase TAO1, in three individuals with NDDs but not in persons who did not have NDDs. Through further screening and the use of GeneMatcher, five additional individuals with NDDs were found to have *de novo* variants. All eight variants were absent from gnomAD (Genome Aggregation Database). The variant carriers shared a non-specific phenotype of developmental delay, and six individuals had additional muscular hypotonia. We established a fibroblast line of one mutation carrier, and we demonstrated that reduced mRNA levels of *TAOK1* could be increased upon cycloheximide treatment. These results indicate nonsense-mediated mRNA decay. Further, there was neither detectable phosphorylated TAO1 kinase nor phosphorylated tau in these cells, and mitochondrial morphology was altered. Knockdown of the ortholog gene *Tao1* (Tao, CG14217) in *Drosophila* resulted in delayed early development. The majority of the *Tao1*-knockdown flies did not survive beyond the third instar larval stage. When compared to control flies, *Tao1* knockdown flies revealed changed morphology of the ventral nerve cord and the neuromuscular junctions as well as a decreased number of endings (boutons). Furthermore, mitochondria in mutant flies showed altered distribution and decreased size in axons of motor neurons. Thus, we provide compelling evidence that *de novo* variants in *TAOK1* cause NDDs.

Approximately 2%–5% of children are born with major congenital malformations,[1] which are often accompanied by neurodevelopmental disorders (NDDs) with variable severity and different behavioral abnormalities. Of note, NDDs often arise from pathogenic *de novo* variants in genes critical for brain development.[2,3] As a result of the enormous genetic heterogeneity of these disorders, next-generation sequencing approaches have been effective means of diagnosing individuals with NDDs, but the diagnostic yield is about 50% at best.[4] The molecular diagnosis provides an approach to shifting from a more phenotype-driven management of the symptoms to a more refined treatment based on genotype.[5]

To further elucidate the genetic spectrum of NDDs, we analyzed exome sequencing data from 4,785 patient-parent trios that were referred to Centogene AG (Rostock, Germany) for diagnostic exome sequencing in the period between January 2014 and June 2017. Most of the individuals with NDDs originated from the Middle East (64%) and from Europe (21%). Clinical information was provided by the referring physicians. These trios included 2,030 individuals with some form of NDD (as defined by the Human Phenotype Ontology [HPO] nomenclature[6,7]: global developmental delay, seizures, microcephaly, macrocephaly, motor delay, delayed speech and language development, or intellectual disability). The remaining 2,755 trios were comprised of persons with other diseases. Written informed consent was obtained from affected individuals and/or guardians after the benefits and risks of clinical exome sequencing testing were explained to them. This study was approved by the Ethical Commission of the faculty of Medicine of the University of Rostock, Germany (registry no. A2015-0102). The samples were processed in Centogene's laboratory (see Supplemental Data). Sequencing data were filtered for good quality (mean sequencing depth of >100×) and variants were only

[1]Institute of Neurogenetics, University of Lübeck, 23538 Lübeck, Germany; [2]Centogene AG, 18055 Rostock, Germany; [3]Department of Medical Genetics, Telemark Hospital Trust, 3710 Skien, Norway; [4]Institute of Clinical Genetics, Technical University of Dresden, Dresden, Germany; [5]Research Unit for Pediatrics, Pediatric Neurology, Pediatric Surgery, Child Psychiatry, Dermatology, Clinical Genetics, Obstetrics and Gynecology, Otorhinolaryngology and Ophthalmology (PEDEGO Research Unit) and Medical Research Center Oulu, University of Oulu and Oulu University Hospital, 90029 OYS Oulu, Finland; [6]Department of Clinical Genetics, Oulu University Hospital, 90029 OYS Oulu, Finland; [7]Institute of Human Genetics, University Hospital Leipzig, 04103 Leipzig, Germany; [8]Center for Pediatric Research Leipzig, Department of Women and Child Health, Hospital for Children and Adolescents, University Hospitals, 04103 Leipzig, Germany; [9]Department of Pediatric Services, Johns Hopkins Aramco Health Care, 34465 Dharan, Saudi Arabia; [10]Pronto Diagnostics, 6158002 Tel Aviv, Israel; [11]Department of Pathology and Laboratory Medicine, College of Medicine, King Saud bin Abdulaziz University for Health Sciences, King Abdullah International Medical Research Center, King Abdulaziz Medical City, 11426 Riyadh, Saudi Arabia; [12]University of Rostock, 18147 Rostock, Germany
[13]These authors contributed equally to this work
*Correspondence: katja.lohmann@neuro.uni-luebeck.de
https://doi.org/10.1016/j.ajhg.2019.05.005.

Table 1. List of Variants Identified in *TAOK1* in This Study

Individual	Chr	Position (GRCh37/hg19)	Ref	Alt	cDNA (GenBank: NM_020791.2)	Protein (GenBank: NP_065842.1)	Country of Origin	Sex	CADD score[12] (v1.4)	*De Novo*	GnomAD	ACMG Scoring[38]	Pathogenicity
Initial Exome Screening													
1	17	27778616	A	G	c.50A>G	p.Glu17Gly	SA	F	23.2	yes	not reported	PS2, PM2	likely path
2	17	27822638	A	G	c.892A>G	p.Lys298Glu	Israel	M	27	yes	not reported	PS2, PM2	likely path
3	17	27857617	G	T	c.2341G>T	p.Glu781*	SA	M	42	yes	not reported	PVS1, PS2, PM2	path
Additional Carriers (Centogene)													
4	17	27822660	A	C	c.914A>C	p.Asp305Ala	Israel	F	27.6	yes	not reported	PS2, PM2	likely path
5	17	27837936	C	T	c.1630C>T	p.Gln544*	Finland	M	38	yes	not reported	PVS1, PS2, PM2	path
Additional Carriers (GeneMatcher)													
6	17	27804704	C	T	c.332C>T	p.Ser111Phe	Germany	F	26.8	yes	not reported	PS2, PM2	likely path
7	17	27861140	G	GC	c.2366_2367insC	p.Leu790Phefs*3	Norway	M	35	yes	not reported	PVS1, PS2, PM2	path
8	17	27861262	G	T	c.2488G>T	p.Glu830*	Germany	M	46	yes	not reported	PVS1, PS2, PM2	path

Abbreviations are as follows: Chr—chromosome, Ref—reference allele, Alt—alternate allele, *De novo*—parents available to confirm de novo status, SA—Saudi Arabia, likely path—likely pathogenic, and path—pathogenic.

considered if the sequencing depth was >20×, the variant allele fraction was >20% of called reads, and the quality Phred score was >220. We performed Sanger sequencing validations for all variants with quality Phred scores <300 to rule out false-positive variants, as previously described.[8]

The frequency of *de novo* variants was compared between the 2,030 NDD and the 2,755 non-NDD trios in the 3,230 genes with a pLI score (the probability of being loss-of-function [LoF] intolerant) of ≥0.9, which indicated a high intolerance to LoF variants.[9] The gene with the highest difference in the occurrence of *de novo* changes was *TAOK1* (thousand and one amino acid [TAO] kinase 1, MIM: 610266, pLI = 1.00), which encodes the serine/threonine-protein kinase TAO1, which is highly expressed in the brain.[10] We detected three *de novo* changes in *TAOK1* among the NDD trios (individuals 1–3) but none in the non-NDD individuals ($p = 0.08$, Fisher's exact test). The *de novo* variants included two missense (c.50A>G [p.Glu17Gly], c.892A>G [p.Lys298Glu]), and one nonsense change (c.2341G>T [p.Glu781*])(GenBank: NM_020791.2).

In a next step, we specifically searched for *TAOK1 de novo* variants in 1,719 NDD patient-parent trios that were more recently (between July 2017 and February 2019) referred to Centogene AG for diagnostic exome sequencing. This revealed two additional carriers (individuals 4 and 5) of a missense (c.914A>C [p.Asp305Ala]) and a nonsense (c.1630C>T [p.Gln544*]) variant.

Finally, three additional individuals with *de novo* variants in *TAOK1* were identified through GeneMatcher[11] (individual 6, c.332C>T [p.Ser111Phe]; individual 7, c.2366_2367insC [p.Leu790Phefs*3]; and individual 8, c.2488G>T [p.Glu830*]) (Table 1, Figure 1, Supplemental Data). These individuals were sequenced in a diagnostic setting at the University of Leipzig (individual 6); at Telemark Hospital Trust, Norway (individual 7); or at the Technical University of Dresden, Germany (individual 8) according to standard procedures.

All eight *TAOK1* variants were *in silico* predicted to be pathogenic (CADD [Combined Annotation Dependent Depletion] score[12] >20) and not reported in gnomAD (Genome Aggregation Database) (Table 1).

Phenotypically, all eight variant carriers had developmental delay affecting speech and language development and/or motor development. Furthermore, muscular hypotonia was present in six, and intellectual disability was present in four individuals. Abnormal facial shape was found in five variant carriers, three of whom also had macrocephaly. Several other abnormalities were reported only in one or two individuals, and it is still unclear whether these signs and symptoms belong to the phenotypic spectrum (for details, see Table S1). Only one of the individuals had seizures. Individual 8 carried an additional *de novo* variant in *FBN1* (MIM: 134797). This person also had features of Marfan syndrome (MIM: 154700) including congenital club feet, retrognathia, high palate, and joint

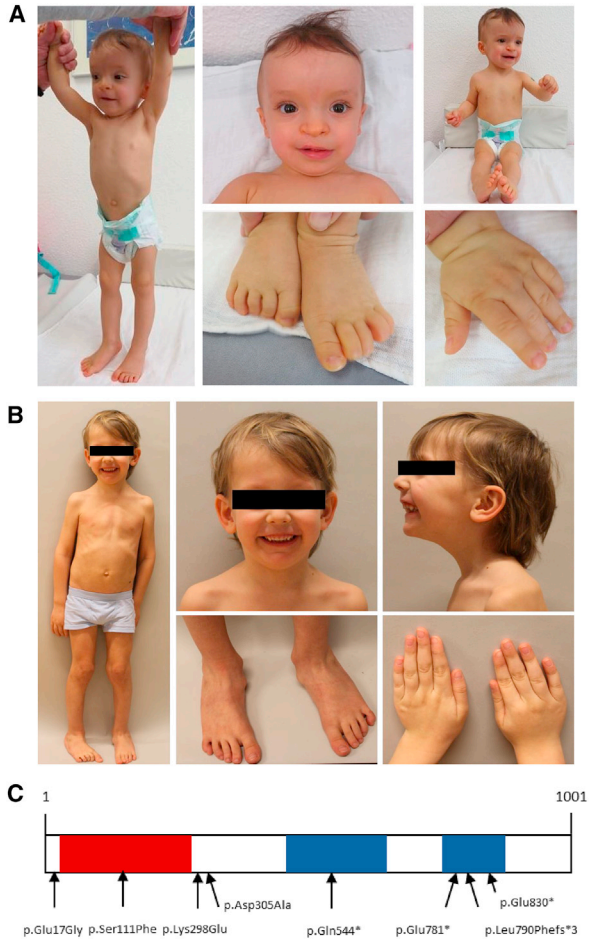

Figure 1. *De novo* Variants in *TAOK1* Detected in Individuals with NDDs

(A) Photographs of individual 6 show dysmorphic features including microsomia with short proximal extremities, macrocephaly with a high forehead, low-set ears, and down-slanting eyelids. The asymmetry of the lips is caused by the surgical intervention to correct the cleft lip and is therefore a secondary phenomenon.

(B) Photographs of individual 8 show dysmorphic features including a long face, a high forehead, big ears, a long nose, down-slanting palpebral fissures, retrognathia, congenital flat feet, and hyperextensibility of the distal joints. The latter three features might be linked to the *FBNI* mutation and fit the diagnosis of Marfan syndrome.

(C) Schematic representation of the encoded TAO1 kinase with its 1,001 amino acids. The functional domains (protein kinase [amino acids 28–281] and coiled-coil motifs 1 [amino acids 458–651] and 2 [amino acids 754–877]) are highlighted in red and blue, respectively. Arrows indicate the locations of the detected variants (see Table 1 for further descriptions). GenBank: NM_020791.2; NP_065842.1.

laxity. (Because of the relation between these features and the *FBN1* variant, these findings have not been included in Table S1.)

The frequency of carriers of *de novo* variants among our 3,749 NDD trios was 0.13%; the carriers included three carriers of *de novo* missense variants and two carriers of truncating variants. In gnomAD, a total of 12 carriers of LoF variants, all heterozygous and spread over the gene, are listed among the about 140,000 sequenced individuals (0.009%). Of note, it is not confirmed that these variants are real nor is there information about whether they occurred *de novo* or about the phenotype of the carriers. The gnomAD consortium removed individuals known to be affected by severe pediatric disease from the database; however, it should be noted that some individuals with severe disease might still be included in the dataset, albeit most likely at a frequency equivalent to or lower than that seen in the general population, as stated at the gnomAD homepage. Comparing the frequency of truncating variants in our samples (0.05%) and in gnomAD (0.009%) reveals a significantly higher rate of truncating variants among the individuals with NDDs ($p = 0.049$, Fisher's exact test) than among those without. In addition, there are 163 unique missense variants listed in gnomAD, and the Z score for missense variants (a measurement of the deviation of observed missense variants from expectations)[13] in *TAOK1* is 4.92, suggesting a pathogenic role for at least a subset of missense variants. At this stage, functional consequences cannot be confirmed for the missense variants located within or near the kinase domain, as found in individuals 1, 2, 4, or 6. However, the phenotypic overlap with other individuals and the *de novo* occurrence support pathogenicity.

For individual 7, RNA could be extracted from a fresh blood sample via a PAXgene tube sampling. We also included three healthy, mutation-negative controls. Total RNA was extracted with the PAXgene Blood RNA Kit (QIAGEN) and then reverse transcribed into cDNA through use of the Maxima First Strand cDNA Synthesis Kit (Thermo Scientific). First, we sequenced the *TAOK1* cDNA, which confirmed the expression of the variant but indicated lower levels of the mutant allele than of the wild-type allele (Figure 2A). Second, we performed quantitative PCR with SYBR Green on the LightCycler 480 system (Roche Diagnostics) that revealed *TAOK1* expression of only 20%–45% in individual 7 compared to the controls (Figure 2B) when normalizing to two different reference genes in the blood sample (*ACTB, G6PD*). Next, we established a fibroblast line from individual 7 (L-13908) and extracted RNA by using the QIAmp RNA Extraction Kit (QIAGEN). Oligo(dT) nucleotides from the Maxima First Strand cDNA Synthesis Kit (ThermoFisher) served as primers for synthesis the complementary DNA (cDNA) by use of reverse transcriptase (RT). Expression analyses of *TAOK1* in fibroblasts revealed a level of 20%–30% *TAOK1* in individual 7 compared to the controls. Because this person carries one wild-type allele, the decrease in expression levels is more pronounced than expected. It can be speculated that TAO1 kinase regulates its own expression through a feedback loop. Confirming this hypothesis will require investigations of the expression in additional mutation carriers and elucidation of a potential mechanism. In the fibroblast line from individual 7, the mutated mRNA could be stabilized by cycloheximide treatment (CHX, for 8 h at 100 μg/mL final concentration)

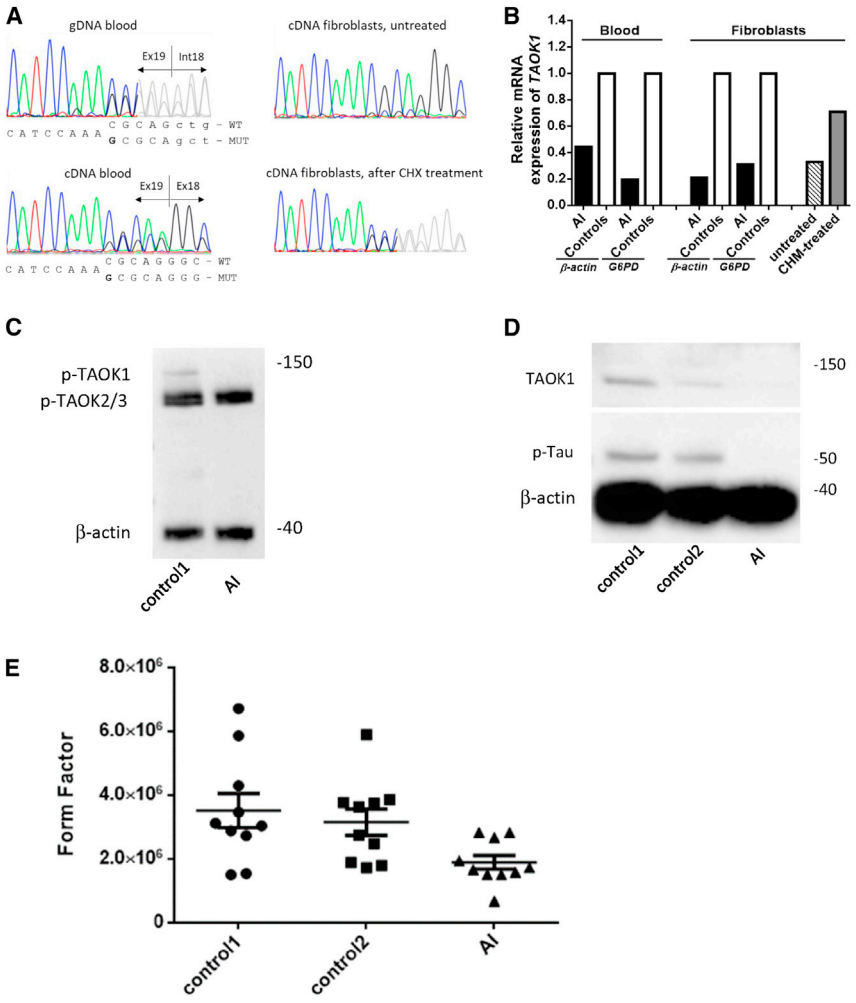

Figure 2. Characterization of the *TAOK1* Variant c.2366_2367insC in Blood and a Fibroblast Line Derived from the Mutation Carrier

(A) Electropherograms of Sanger sequencing of genomic (gDNA) and complementary DNA (cDNA) of individual 7 in the reverse direction. The variant is shown on the genomic level (upper left panel) from a blood sample, and the inserted C (G on the reverse strand) is highlighted. The expression of the mutant allele is decreased in blood (lower left panel), and in the fibroblast line (upper right panel) compared to the wild-type allele, as shown by the lower height of the peaks using Sanger sequencing. The mutant allele could be stabilized upon treatment with cycloheximide (CHX, 100 μg/mL, 8 h) as illustrated in the lower right panel.

(B) The quantification of *TAOK1* mRNA levels by real-time PCR indicated highly reduced levels of *TAOK1* in the affected individual (AI) compared to the control individuals (controls) in blood and fibroblasts. The expression in fibroblasts can be increased upon treatment with cycloheximide (CHX).

(C) Immunoblot analysis of total protein extract from fibroblasts of the affected individual (AI) and a control (control 1) with an antibody against phosphorylated TAO kinases TAO1, TAO2, and TAO3 indicates the absence of detectable, phosphorylated TAO1 kinase (p-TAOK1) in cells of the affected individual. Phosphorylation and abundance of TAO2 and 3 kinases (p-TAOK2/3) seemed to be unaltered. β-actin (ACTIN) was used as a loading control.

(D) Immunoblot analysis of total protein extract from the fibroblast line of the affected individual (AI) and two controls (control 1, control 2) with antibodies against total TAOK1 and phosphorylated tau protein (p-tau) indicating absence of both TAOK1 and p-tau in cells of the affected individual. β-actin (ACTN) was used as a loading control.

(E) Form factor as a measurement for mitochondrial interconnectivity was calculated in the fibroblast line of the affected individual (AI) and two controls (control 1, control 2) (10 cells each). Each dot represents the value in a single cell, and the mean and the interquartile range per individual are indicated.

indicating nonsense-mediated mRNA decay as an explanation for the reduced abundance of the mutant allele (Figures 2A and 2B).

We also performed immunoblotting with total protein extracts from the fibroblast line from individual 7 and two different control fibroblast lines. Antibodies used for immunoblotting were as follows: anti-TAOK3 (phospho S177) + TAOK2 (phospho S181) + TAOK1 (phospho S181) antibody (1:1000; Abcam), anti-TAOK1 (1:1000; Bethyl Laboratories), anti-p-tau (1:1000; Cell Signaling), and anti-β-actin (1:1,000,000; Sigma). This revealed a band for phosphorylated TAO1 kinase only in the control but not in individual 7 indicating loss of detectable phosphorylated TAO1 kinase in the mutated fibroblasts (Figure 2C). Total TAO1 kinase was also not evident in the cells of individual 7 (Figure 2D).

In *Drosophila*, Tao1 has been reported to affect overall brain volume at the mid-third-instar larval stage (L3).[14] Furthermore, mutant Tao1 in *Drosophila* has been demonstrated to negatively regulate Par-1 as part of a signaling pathway in developing neurons, causing defects in the morphology of the central brain.[15] Also, mammalian TAO1 kinase has been shown to phosphorylate and thereby activate PAR-1 (microtubule affinity-regulating kinase[MARK2]), leading in turn to phosphorylation of the mictotubule-stabilizing protein tau; this phosphorylation results in decreased tau affinity for microtubules.[16] Thus, mammalian TAO1 kinase controls the extension of neurites in immature cultured neurons through its effects on the microtubule cytoskeleton.[16,17] Using patient-derived fibroblast cells from individual 7 and two different control fibroblast lines, we performed immunoblotting against phosphorylated tau protein and showed that there was no detectable phosphorylated tau (p-tau) protein in the mutant fibroblasts (Figure 2D). In accordance with previous observations,[18] our results demonstrate that decreased TAO1 kinase protein levels effectively decrease tau phosphorylation in fibroblasts of a *TAOK1* mutation carrier. Notably, higher p-tau levels have been shown to elongate the mitochondria as a result of delocalization of

dynamin related protein 1 (DRP1), the fission protein for mitochondria.[19] Having in mind the decreased levels of p-tau in the fibroblast culture of the affected individual, we speculated that reduced p-tau could result in shorter or smaller mitochondria. Thus, we analyzed the effect of decreased TAO1 kinase levels on the integrity of the mitochondrial network by calculating the form factor in fibroblasts of a *TAOK1* mutation carrier and two unrelated healthy controls (Figure 2E). The form factor as a measure of the integrity of the mitochondrial network was determined as previously described.[20] The form factor analysis revealed a reduction in the degree of mitochondrial branching and interconnectivity in fibroblasts from the affected individual compared to fibroblasts from healthy controls, implicating an impaired mitochondrial network.

Four of the eight *TAOK1* variants that we detected in our individuals result in null alleles as a result of premature protein truncation or decreased expression due to nonsense-mediated mRNA decay, as shown for the c.2366_2367insC variant. To further investigate the consequences of loss of TAO1 kinase and to confirm its role in neurodevelopment, we used two independent *Drosophila melanogaster* RNAi-mediated knockdown lines for Tao1 depletion: the TAO1_GD RNA interference line (17432) and the TAO1_KK RNA interference line (107645) (purchased from the Vienna *Drosophila* Resource Center). Tao1 was ubiquitously knocked down via the Daughterless Gal4 (DaGal4) driver, and w1118 (purchased from the Bloomington *Drosophila* Stock Center) was used as a control line. *Drosophila* Tao1 (Tao, CG14217) is the single representative of the TAO kinase subfamily[21] that is highly similar to all three mammalian TAO kinase family proteins, TAO1, TAO2, and TAO3 (60%–70% identity in the protein kinase domain and 45% identity in the conserved C-terminal domain). All fly experiments were performed at least three times. Compared with controls, both TAO1_KK and TAO1_GD knockdown flies showed delayed development (Figure S1) and early death (discontinued development) between the L3 and the pharate adult (PA) stage (Figure 3A). Furthermore, we used immunostaining to investigate the structure of the ventral nerve cord (VNC), neuromuscular junctions (NMJs), and the NMJs' endings (boutons). Standard dissection and immunostaining procedures were used for larval tissue analysis. For immunocytochemical analysis, larval fillets at the L3 stage were dissected in the physiological solution HL-3[22] then fixed for 20 min in 4% formaldehyde, washed in PBS, permeabilized with 0.4% Triton X-100 dissolved in PBS, and blocked for 1 h with 10% normal goat serum. Larval fillets were incubated overnight with the following primary antibodies: the synaptic marker anti-DLG (1:400; 4F3 anti-Disc large; Developmental Studies Hybridoma Bank) for labeling VNC and NMJs and anti-GABARABAP (1:100; Abcam) for defining muscular structures. The respective secondary antibodies were used: anti-rabbit Alexa Fluor® 488 (1:100; Thermo Fisher Scientific) and anti-mouse Alexa Fluor® 596 (1:100; Thermo Fisher Scientific). The images were taken on a confocal microscope (LSM710; Zeiss). Images of z stacks were examined with ImageJ (NIH software), and the number of boutons per muscle section was counted. At least 15 images from four different larvae were analyzed. Immunostaining of the larval VNC showed a reduction in size of VNC, less-defined structures of VNC, and less-developed axons originating in the VNC in *Tao1* knockdown larvae (Figure 3B). Additionally, immunostaining of the NMJs revealed changed NMJ morphology and a significantly decreased number of boutons per muscle section in *Tao1* knockdown larvae compared to control larvae (Figures 3C and 3D).

Given the changes in the mitochondrial network detected in fibroblasts from individual 7, we further analyzed the effect of decreased Tao1 levels on mitochondrial distribution and size in axons of *Drosophila* with knockdown of *Tao1*. Of note, dysmorphic mitochondria would result in decreased mitochondrial production of ATP, which is essential for the maintenance of axonal transport and function.[23] We crossed control (w1118) and *Tao1* RNAi lines (TAO1_GD) with flies expressing mitochondrial-tagged GFP (mtGFP) predominantly in motor neurons (mtGFP,D42Gal4) (purchased from the Bloomington stock center). mtGFP encodes the S65T spectral variant of GFP fused at the N terminus with the 31-amino-acid mitochondrial import sequence from human cytochrome C oxidase subunit VIII. *Tao1* was ubiquitously knocked down via the D42Gal4 driver, which is predominantly expressed in motor neurons.[24] Standard dissection and fixation procedures were used for the L3 stage larval tissue analysis. Quantification of mitochondrial area per axon (μm^2) was counted from images of z stacks with ImageJ (NIH software). Differences were analyzed statistically using unpaired t tests with a Bonferroni–Dunn post hoc correction. We observed disturbed mitochondrial distribution and significantly decreased average mitochondrial size in axons of *Tao1* knockdown flies compared to the control flies (Figures 3E and 3F), implicating impaired axonal transport and function. These data collectively demonstrate that the effect of knockdown of *Tao1* on early development is characterized by reduction in the number of NMJ endings, the size of the VNC in flies, and the mitochondrial size in axons, confirming that depletion of Tao1 results in neurodevelopmental impairment in *Drosophila*.

NDD is a highly heterogeneous disease group[25] with a large number of biological pathways affected by pathogenic variants, reflecting the complexity of normal brain development. A microdeletion on chromosome 17, comprising *TAOK1,* had nominated *TAOK1* as a potential candidate gene for developmental delay and microcephaly.[26] The Decipher database reports four additional patients with large deletions that include the *TAOK1* gene. These patients include one who has an intragenic deletion of exons 2–8 and a reported phenotype of microcephaly and seizures. We show here multiple sequence variants in persons with NDDs; all of these variants occurred *de novo* and thus support the possibility that these changes are pathogenic and

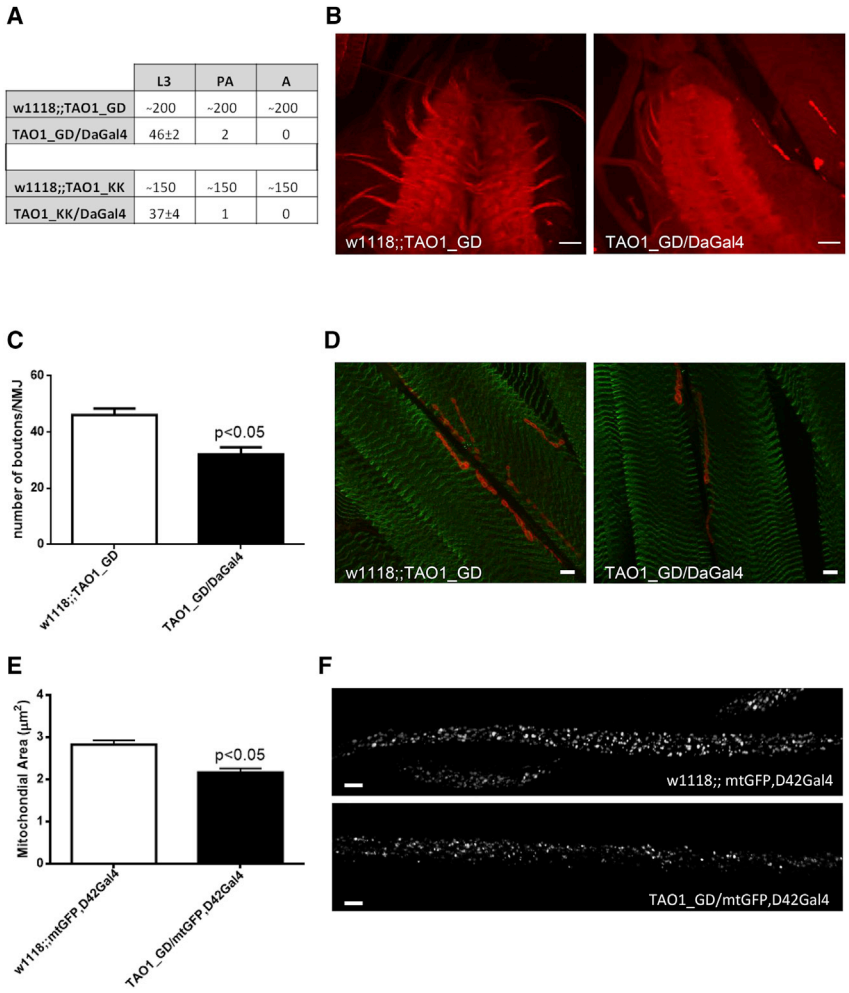

Figure 3. Impaired Neurodevelopment in *Drosophila* with Knockdown of *Tao1*

(A) Early lethality in *Tao1* knockdown flies. The table indicates the number of living flies in different stages (L3 — third instar larvae stage; PA — pharate adult stage; A — adult flies). Two *Tao1* RNAi lines (TAO1_GD and TAO1_KK) were crossed with w1118 control line and the DaGal4 driver, which ubiquitously knocks down *Tao1*.

(B) Smaller-sized ventral nerve cord in *Tao1* knockdown flies. Representative images of L3 control (w1118;;TAO1_GD) and L3 *Tao1* knockdown (TAO1_GD/DaGal4) larval ventral nerve cord (VNC) are shown, indicating a reduction in the size of VNC and less-developed axons starting from VNC in *Tao1* knockdown flies. Immunolabeling of the L3 larval VNC was done with the synaptic marker anti-DLG (red). Four animals per genotype were analyzed. The scale bar represents 20 μm.

(C) Significantly decreased amount of neuromuscular junction endings (boutons) in *Tao1* knockdown flies. Quantification of boutons in control (w1118;;TAO1_GD) and *Tao1* knockdown (TAO1_GD/DaGal4) larvae. $p < 0.05$ — significantly decreased number of boutons compared to those of the control; 15 images from four animals per genotype were analyzed. Error bars represent the SEM.

(D) Representative images of the neuromuscular junctions and boutons are shown, indicating changed morphology and a reduced number of boutons. Immunolabeling of L3 control (w1118;;TAO1_GD) and L3 *Tao1* knockdown (TAO1_GD/DaGal4) larval neuromuscular junctions (NMJs) and their boutons with the synaptic marker anti-DLG (red) and anti-GABARAB (green) defined muscular structure. The scale bar represents 10 μm.

(E) Significantly decreased average mitochondrial size (μm^2) in axons of *Tao1* knockdown flies. The control line (w1118) and *Tao1* RNAi line (TAO1_GD) were crossed with flies expressing mitochondrial-tagged GFP, predominantly in the motor neurons (mtGFP,D42Gal4), and quantification of axonal mitochondrial area in control (w1118;;mtGFP,D42Gal4) and *Tao1* knockdown (TAO1_GD/mtGFP,D42Gal4) L3 larvae is shown. $p < 0.05$ — significantly decreased average mitochondrial area compared to the control; 10 images from three animals per genotype were analyzed. Error bars represent the SEM.

(F) Representative images of axonal mitochondria are shown, indicating disturbed mitochondrial distribution and reduced mitochondrial size. The scale bar represents 10 μm.

that *TAOK1* plays a role in NDDs. TAO1 kinase was shown to induce microtubule instability via activation of microtubule affinity-regulating kinase (MARK) and phosphorylation of microtubule-associated proteins, including tau, whose dissociation from microtubules results in microtubule disassembly.[15,27] Altered microtubule stability in maturing neurons could potentially lead to a perturbed neuronal network.[28] Notably, previous studies have shown that pathogenic variants in a number of tubulin subunits, including *TUBB2B* (MIM: 612850), *TUBB3* (MIM: 602661), and *TUBG1* (MIM: 191135), cause brain malformations and NDDs.[29–32] These findings link different NDDs on the molecular level. Additionally, *TAOK1* is activated during microtubule-dependent processes such as mitosis and neuritogenesis, and knockdown of *TAOK1* expression inhibits these processes.[27,33] Furthermore, TAO1 kinase was previously implicated as an important regulator of checkpoint control because it caused the most penetrant checkpoint defect.[34] Its dual function in regulating microtubule dynamics and mitotic progression contributes to correct congression of chromosomes, thereby protecting genomic stability in human cells. During neuronal development, an impaired congression of chromosomes during mitosis would lead to an altered proportion of symmetrical and asymmetrical progenitor cell division. This effect could be further enhanced by down-regulation of the G2/M checkpoint as a result of TAO1 kinase loss,[35] leading to reduced apoptosis.[36] Apoptosis is a necessary mechanism of programmed cell death during neuronal development and differentiation.[37]

Thus, through controlling the extension of neurites in immature cultured neurons,[16,17] through its role in the regulation of tau phosphorylation and dissociation from microtubules,[16,17,32] and through congression of

chromosomes during mitosis,[34] TAO1 kinase plays a role in the establishment of neuronal polarity, neuronal differentiation, and early brain development. These molecular mechanisms could play an essential role in impaired brain development in *TAOK1* mutation carriers. Accordingly, Tao1 kinase has been shown to affect the size of the larval brain in *Drosophila*,[14] and mutations in *Tao1* cause defects in the morphology of the central brain in flies.[15]

In conclusion, we provide strong genetic and functional support that LoF variants in *TAOK1* are an additional cause of NDDs.

Supplemental Data

Supplemental Data can be found online at https://doi.org/10.1016/j.ajhg.2019.05.005.

Acknowledgments

We would like to thank the participants and Eli Ormerod (Oslo University Hospital) for establishing the cell line from individual 7. The study was funded by the University of Lübeck. Exome sequencing was done as part of diagnostic work-up.

Declaration of Interests

G. Oprea, M. Werber, and A. Rolfs are employees and shareholders of Centogene AG. R. Affan is an employee and shareholder of Pronto Diagnostics. A. Rolfs is a founder of Centogene AG and a member of its scientific advisory board. N. Navot is a founder of Pronto Diagnostics and a member of its scientific advisory board. S. Kishore is a founder of his own startup, Mimamsia, and is the primary shareholder of this company (after his contribution to this manuscript and thus unrelated to this manuscript). The remaining authors declare no competing interests. None of the authors is member of a board or advisory committee or a paid consultant in relation to this study or holds any patent related to this work.

Received: January 8, 2019
Accepted: May 8, 2019
Published: June 20, 2019

Web Resources

CADD score, https://cadd.gs.washington.edu/score
DECIPHER, https://decipher.sanger.ac.uk/search?q=TAOK1#consented-patients/results
GeneMatcher, https://genematcher.org/
GnomAD, https://gnomad.broadinstitute.org/gene/ENSG00000160551
OMIM, https://omim.org/
Transcript (GenBank: NP_065842), https://www.ncbi.nlm.nih.gov/nuccore/NM_020791
UniProt, https://www.uniprot.org/
Vienna *Drosophila* Resource Center, https://stockcenter.vdrc.at/control/main

References

1. Sheridan, E., Wright, J., Small, N., Corry, P.C., Oddie, S., Whibley, C., Petherick, E.S., Malik, T., Pawson, N., McKinney, P.A., and Parslow, R.C. (2013). Risk factors for congenital anomaly in a multiethnic birth cohort: an analysis of the Born in Bradford study. Lancet *382*, 1350–1359.
2. Hoischen, A., Krumm, N., and Eichler, E.E. (2014). Prioritization of neurodevelopmental disease genes by discovery of new mutations. Nat. Neurosci. *17*, 764–772.
3. Ku, C.S., Polychronakos, C., Tan, E.K., Naidoo, N., Pawitan, Y., Roukos, D.H., Mort, M., and Cooper, D.N. (2013). A new paradigm emerges from the study of de novo mutations in the context of neurodevelopmental disease. Mol. Psychiatry *18*, 141–153.
4. Wright, C.F., McRae, J.F., Clayton, S., Gallone, G., Aitken, S., FitzGerald, T.W., Jones, P., Prigmore, E., Rajan, D., Lord, J., et al.; DDD Study (2018). Making new genetic diagnoses with old data: iterative reanalysis and reporting from genome-wide data in 1,133 families with developmental disorders. Genet. Med. *20*, 1216–1223.
5. Aronson, S.J., and Rehm, H.L. (2015). Building the foundation for genomics in precision medicine. Nature *526*, 336–342.
6. Robinson, P.N., Köhler, S., Bauer, S., Seelow, D., Horn, D., and Mundlos, S. (2008). The Human Phenotype Ontology: A tool for annotating and analyzing human hereditary disease. Am. J. Hum. Genet. *83*, 610–615.
7. Groza, T., Köhler, S., Moldenhauer, D., Vasilevsky, N., Baynam, G., Zemojtel, T., Schriml, L.M., Kibbe, W.A., Schofield, P.N., Beck, T., et al. (2015). The Human Phenotype Ontology: Semantic unification of common and rare disease. Am. J. Hum. Genet. *97*, 111–124.
8. Trujillano, D., Bertoli-Avella, A.M., Kumar Kandaswamy, K., Weiss, M.E., Köster, J., Marais, A., Paknia, O., Schröder, R., Garcia-Aznar, J.M., Werber, M., et al. (2017). Clinical exome sequencing: Results from 2819 samples reflecting 1000 families. Eur. J. Hum. Genet. *25*, 176–182.
9. Lek, M., Karczewski, K.J., Minikel, E.V., Samocha, K.E., Banks, E., Fennell, T., O'Donnell-Luria, A.H., Ware, J.S., Hill, A.J., Cummings, B.B., et al.; Exome Aggregation Consortium (2016). Analysis of protein-coding genetic variation in 60,706 humans. Nature *536*, 285–291.
10. Hutchison, M., Berman, K.S., and Cobb, M.H. (1998). Isolation of TAO1, a protein kinase that activates MEKs in stress-activated protein kinase cascades. J. Biol. Chem. *273*, 28625–28632.
11. Sobreira, N., Schiettecatte, F., Valle, D., and Hamosh, A. (2015). GeneMatcher: A matching tool for connecting investigators with an interest in the same gene. Hum. Mutat. *36*, 928–930.
12. Kircher, M., Witten, D.M., Jain, P., O'Roak, B.J., Cooper, G.M., and Shendure, J. (2014). A general framework for estimating the relative pathogenicity of human genetic variants. Nat. Genet. *46*, 310–315.
13. Samocha, K.E., Robinson, E.B., Sanders, S.J., Stevens, C., Sabo, A., McGrath, L.M., Kosmicki, J.A., Rehnström, K., Mallick, S., Kirby, A., et al. (2014). A framework for the interpretation of de novo mutation in human disease. Nat. Genet. *46*, 944–950.
14. Poon, C.L., Mitchell, K.A., Kondo, S., Cheng, L.Y., and Harvey, K.F. (2016). The hippo pathway regulates neuroblasts and brain size in Drosophila melanogaster. Curr. Biol. *26*, 1034–1042.
15. King, I., Tsai, L.T., Pflanz, R., Voigt, A., Lee, S., Jäckle, H., Lu, B., and Heberlein, U. (2011). Drosophila tao controls mushroom body development and ethanol-stimulated behavior through par-1. J. Neurosci. *31*, 1139–1148.

16. Timm, T., Matenia, D., Li, X.Y., Griesshaber, B., and Mandelkow, E.M. (2006). Signaling from MARK to tau: regulation, cytoskeletal crosstalk, and pathological phosphorylation. Neurodegener. Dis. *3*, 207–217.
17. Biernat, J., Wu, Y.Z., Timm, T., Zheng-Fischhöfer, Q., Mandelkow, E., Meijer, L., and Mandelkow, E.M. (2002). Protein kinase MARK/PAR-1 is required for neurite outgrowth and establishment of neuronal polarity. Mol. Biol. Cell *13*, 4013–4028.
18. Giacomini, C., Koo, C.Y., Yankova, N., Tavares, I.A., Wray, S., Noble, W., Hanger, D.P., and Morris, J.D.H. (2018). A new TAO kinase inhibitor reduces tau phosphorylation at sites associated with neurodegeneration in human tauopathies. Acta Neuropathol. Commun. *6*, 37.
19. Perez, M., Jara, C., and Quintanilla, R.A. (2018). Contribution of Tau Pathology to Mitochondrial Impairment in Neurodegeneration. Front. Neurosci. *12*, 441.
20. Grünewald, A., Voges, L., Rakovic, A., Kasten, M., Vandebona, H., Hemmelmann, C., Lohmann, K., Orolicki, S., Ramirez, A., Schapira, A.H., et al. (2010). Mutant Parkin impairs mitochondrial function and morphology in human fibroblasts. PLoS ONE *5*, e12962.
21. Dan, I., Watanabe, N.M., and Kusumi, A. (2001). The Ste20 group kinases as regulators of MAP kinase cascades. Trends Cell Biol. *11*, 220–230.
22. Uytterhoeven, V., Kuenen, S., Kasprowicz, J., Miskiewicz, K., and Verstreken, P. (2011). Loss of skywalker reveals synaptic endosomes as sorting stations for synaptic vesicle proteins. Cell *145*, 117–132.
23. Ochs, S., and Hollingsworth, D. (1971). Dependence of fast axoplasmic transport in nerve on oxidative metabolism. J. Neurochem. *18*, 107–114.
24. Sanyal, S. (2009). Genomic mapping and expression patterns of C380, OK6 and D42 enhancer trap lines in the larval nervous system of Drosophila. Gene Expr. Patterns *9*, 371–380.
25. Platzer, K., Sticht, H., Edwards, S.L., Allen, W., Angione, K.M., Bonati, M.T., Brasington, C., Cho, M.T., Demmer, L.A., Falik-Zaccai, T., et al. (2019). De novo variants in MAPK8IP3 cause intellectual disability with variable brain anomalies. Am. J. Hum. Genet. *104*, 203–212.
26. Xie, B., Fan, X., Lei, Y., Chen, R., Wang, J., Fu, C., Yi, S., Luo, J., Zhang, S., Yang, Q., et al. (2016). A novel de novo microdeletion at 17q11.2 adjacent to NF1 gene associated with developmental delay, short stature, microcephaly and dysmorphic features. Mol. Cytogenet. *9*, 41.
27. Timm, T., Li, X.Y., Biernat, J., Jiao, J., Mandelkow, E., Vandekerckhove, J., and Mandelkow, E.M. (2003). MARKK, a Ste20-like kinase, activates the polarity-inducing kinase MARK/PAR-1. EMBO J. *22*, 5090–5101.
28. Chakraborti, S., Natarajan, K., Curiel, J., Janke, C., and Liu, J. (2016). The emerging role of the tubulin code: From the tubulin molecule to neuronal function and disease. Cytoskeleton (Hoboken) *73*, 521–550.
29. Jaglin, X.H., Poirier, K., Saillour, Y., Buhler, E., Tian, G., Bahi-Buisson, N., Fallet-Bianco, C., Phan-Dinh-Tuy, F., Kong, X.P., Bomont, P., et al. (2009). Mutations in the beta-tubulin gene TUBB2B result in asymmetrical polymicrogyria. Nat. Genet. *41*, 746–752.
30. Poirier, K., Lebrun, N., Broix, L., Tian, G., Saillour, Y., Boscheron, C., Parrini, E., Valence, S., Pierre, B.S., Oger, M., et al. (2013). Mutations in TUBG1, DYNC1H1, KIF5C and KIF2A cause malformations of cortical development and microcephaly. Nat. Genet. *45*, 639–647.
31. Poirier, K., Saillour, Y., Bahi-Buisson, N., Jaglin, X.H., Fallet-Bianco, C., Nabbout, R., Castelnau-Ptakhine, L., Roubertie, A., Attie-Bitach, T., Desguerre, I., et al. (2010). Mutations in the neuronal ß-tubulin subunit TUBB3 result in malformation of cortical development and neuronal migration defects. Hum. Mol. Genet. *19*, 4462–4473.
32. Breuss, M., and Keays, D.A. (2014). Microtubules and neurodevelopmental disease: the movers and the makers. Adv. Exp. Med. Biol. *800*, 75–96.
33. Wojtala, R.L., Tavares, I.A., Morton, P.E., Valderrama, F., Thomas, N.S., and Morris, J.D. (2011). Prostate-derived sterile 20-like kinases (PSKs/TAOKs) are activated in mitosis and contribute to mitotic cell rounding and spindle positioning. J. Biol. Chem. *286*, 30161–30170.
34. Draviam, V.M., Stegmeier, F., Nalepa, G., Sowa, M.E., Chen, J., Liang, A., Hannon, G.J., Sorger, P.K., Harper, J.W., and Elledge, S.J. (2007). A functional genomic screen identifies a role for TAO1 kinase in spindle-checkpoint signalling. Nat. Cell Biol. *9*, 556–564.
35. Raman, M., Earnest, S., Zhang, K., Zhao, Y., and Cobb, M.H. (2007). TAO kinases mediate activation of p38 in response to DNA damage. EMBO J. *26*, 2005–2014.
36. Wu, M.F., and Wang, S.G. (2008). Human TAO kinase 1 induces apoptosis in SH-SY5Y cells. Cell Biol. Int. *32*, 151–156.
37. Pinto-Teixeira, F., Konstantinides, N., and Desplan, C. (2016). Programmed cell death acts at different stages of Drosophila neurodevelopment to shape the central nervous system. FEBS Lett. *590*, 2435–2453.
38. Richards, S., Aziz, N., Bale, S., Bick, D., Das, S., Gastier-Foster, J., Grody, W.W., Hegde, M., Lyon, E., Spector, E., et al.; ACMG Laboratory Quality Assurance Committee (2015). Standards and guidelines for the interpretation of sequence variants: a joint consensus recommendation of the American College of Medical Genetics and Genomics and the Association for Molecular Pathology. Genet. Med. *17*, 405–424.